Murine atherosclerotic plaque imaging with the USPIO Ferumoxtran-10

Klug, Gert[1], Kampf Thomas[2], Ziener Christan[2], Parczyk Marco [2], Bauer Elisabeth [1], Herold Volker[2], Rommel, Eberhard[2], Jakob Michael Peter[2], Bauer Rudolf Wolfgang[1]

[1]*Medizinische Klinik und Poliklinik I, Universitaetsklinik Wuerzburg, Germany,*[2] *Experimentelle Physik 5, Universitaet Wuerzburg, Germany*

TABLE OF CONTENTS

1. ABSTRACT

In this study we intended to image plaque inflammation in a murine model of atherosclerosis with MRI and Ferumoxtran-10 (Sinerem®, Guerbet, France). 8 apoE$^{-/-}$ mice were injected 500µmol Fe/kg or 1000µmol Fe/kg Ferumoxtran-10. 2 apoE$^{-/-}$ mice were injected NaCl. After a post-contrast time of 24 to 336 hours the mice were scarificed and the aortas were imaged *ex vivo*. All measurements were performed on a 17.6 Tesla Bruker AVANCE 750WB MR scanner (Bruker, Germany). Spin-echo sequences and gradient-echo sequences with variable TE were performed and T2* maps were generated. Prussian-blue and hematoxilin-eosin histology were obtained afterwards and iron-uptake was quantified by counting iron positive areas. 2 apoE$^{-/-}$ mice were imaged *in vivo* before and 48 hours after 1000µmolFe/kg. Atheroma iron uptake was not elevated after 24 hours compared to controls. 48 hours after 1000µmol Fe/kg but not 500µmol Fe/kg histology revealed a 1.3- fold increase in plaque iron content compared to NaCl injected mice. Normalized T2*-times decreased from 0.86±0.02 in controls to 0.66±0.15 after a dose of 500µmolFe/ml and 0.59±0.14 in mice injected with 1000µmol Fe/Kg (p=0.038). These results translated into a mean of 122% increase in CNR, as measured by *in vivo* MRI. We have demonstrated that Ferumoxtran-10 is taken up by atherosclerotic plaques in untreated apoE$^{-/-}$ mice and this alters plaque signal properties.

2. INTRODUCTION

Estimations of monocytes recruitment into atherosclerosis in Apolipoprotein-E knock-out (apoE$^{-/-}$) mice with the use of superparamagnetic iron-oxide nanoparticles (SPIOs) has been shown to be feasible recently (1).

Because of predominately T2 and T2* shortening effects, USPIOs are primarily used as "negative" contrast agents. Whereas USPIOs molar relaxivities (r1 and r2) decrease with intracellular uptake compared to dissolved contrast medium (2) r2* increases under these conditions (3). This behaviour was predicted by theoretical analysis (3-5) as well as numerical calculations (6). Thus these characteristics are mostly exploited with the use of T2* sensitive gradient-echo sequences to image USPIO uptake (7, 8).

ApoE$^{-/-}$ mice are a popular animal model for atherosclerosis as they develop different stages of atherosclerosis similar to that observed in humans.Previous studies have shown analogies in lesion development, complex morphology and immunophenotype (9, 10). The use of mouse models in atherosclerosis research has the advantages of rapid plaque progression, low maintenance costs and the possibility of further genetical engineering.

Only one study describes the use of untargeted magneto-optical iron-oxide particles without attached

antibodies in apoE [−/−] (7) but the used particles are not commercially available. However the use of USPIOs which are designed for clinical use is of special interest regarding human and pre-clinical applications. Lately one report used the USPIO Sinerem® (Ferumoxtran-10, Guerbet, France) in visualising inflammation in murine atheromas after the chronic administration of angiotensin II to enhance plaque macrophages content (11).

Those studies use different doses and post-contrast times and so far no evaluation of different doses and incubation times on plaque visualization with untargeted (unfunctionalized) and potential clinically applicable USPIOs has been performed in the apoE^{−/−} mouse model of human atherosclerosis.

We intended to study the effects of USPIO dose and incubation times on the tissue contrast properties in the aortic roots of untreated apoE^{−/−} mice with the use of Ferumoxtran-10.

2. MATERIALS AND METHODS

2.1. Animals

A total of 10 apoE [−/−] mice (mean age: 9.1±1.0 months, range: 7.1-9.6 months) (from Charles River, Jackson Mice, Belgium) on normal chow were investigated. 8 apoE [−/−] received Ferumoxtran-10 (Sinerem®, Guerbet, France) at doses of 500 or 1000 μmolFe per kilogramm bodyweight by injection in the tail vein of constant volume of 0.2 ml. The contrast agent was reconstituted in 10 mL saline as recommended by the manufacturer to archive a 360mM Fe solution. Immediately before injection the agent was diluted in 0.9% saline with respect to the weight of the mice. 2 apoE [−/−] were injected 0.2ml of 0.9% NaCl without contrast medium. After a post-contrast time of 24, 48, 168 and 336 hours, mice (two each timepoint) were scarified and the aortas and the heart were removed and fixed in 4% formalin for at least 24 hours. *Ex vivo* MRI was performed within 6 days after removal. Afterwards aortas were placed in KCl for at least 24 hours, dehydrated, embedded, sectioned and stained with a standard hematoxilin/eosin stain as well with a modified Prussian-blue staining.

After those initial experiments 2 apoE [−/−] received 1000μmol Fe/kg BW Ferumoxtran-10 and were imaged ~2 days before and >48 hours after the administration of the contrast agent.

All experiments were performed in accordance with the *Rules and Regulations of NIH and Their Institutions*.

2.2. *ex vivo* MRI

Specimens were washed and perfused with Fomblin (perfluoropolyether, CF3-[(O-CF-CF2)n-(O-CF2)m]-OCF3, Solvay Solexis, Italy) and placed in a 10-mm polyethylene tube filled with Fomblin. Imaging was performed on a 750 MHz (17.6 Tesla) AVANCE wide bore scanner (Bruker BioSpin MRI GmbH, Ettlingen, Germany). Imaging protocol contained T2- to proton-

density (PD)-weighted multi-spin-echo sequences (TR: 2000 [ms], TE: 8.2-42 [ms], in plane resolution 38x38 μm^2, slice thickness: 0.6 [mm], number of averages (NA): 16) to obtain morphological information. 10 slices were adjusted perpendicular to the ascending aorta and reached from beneath the aortic root to above the outlet of the carotid arteries. For T2* evaluation single-slice T2*-weighted gradient-echo (TR: 140 [ms]) sequences with variable TEs ranging from 1.1 [ms] to 30 [ms] were obtained from the aortic root, according to the spin-echo images.

2.3. *in vivo* MRI

After completion of initial studies we performed *in vivo* imaging of 2 apoE [−/−] mice. The MR protocol contained a multi-spin-echo (TR/TE: ~1000/8.2-40 [ms], in plane resolution: 78x78μm², NA: 4) and T2*-weighted gradient-echo sequences (TR: 1 heart beat, TE: 1.1ms, FA: 30˚, in plane resolution: 78x78μm², slice thickness: 500μm, NA: 8) similar to those described above.

2.4. Histological analysis

For easy coregistration of MR-images and histological sections we chose the aortic root as a reference point. Each 50μm a 5μm section was taken from the paraffin embedded aortas and stained with either hematoxilin/eosin or Prussian-blue staining. Hence we matched 4 Prussian-blue stained slides with the corresponding MR slices. On each slide each of the three plaque areas sourounding the aortic valves was analysed in a blinded fashion by one observer with up to five high-power-fields (100x magnification, see Figure 1.: insert). Iron positive areas were counted using a counting grid (10x10). Iron positive squares were counted and their percentage of total high-power-fields was calculated. Macrophage staining was performed in a separate group of age-matched mice with MAC-3 diaminobenzidin immunohistochemestry.

2.5. MR images analysis

T2*-maps were generated based on the variable TE gradient-echo images with an in-house written MATLAB® (The MathWorks Inc. Natwick, MA, USA) routine. Mean T2* times for each plaque segment were evaluated by manual contouring of the aortic root plaque area visually, based on the plaque area on spin-echo images. Plaque-T2* times were expressed relatively to the myocardium via:

$$T2*_{normalized} = \frac{T2*_{Plaque}\,[ms]}{T2*_{Myocardium}\,[ms]}$$

to correct for external field-inhomogeneities. Normalized T2* times are therefore ratios that have no units.

CNR was determined based on signal intensities of *in vivo* T2*-weighted images within the aortic blood volume and the aortic root plaque-area. We chose a TE of 1.1 ms to optimize image quality. Signal intensities were measured on DICOM files by using a manual region-of-interest (ROI) tracing tool (JiveX, VISUS Technology Transfer, Bochum, Germany). The plaque ROI in the aortic root was manually defined according to the plaque area on the high-resoluti
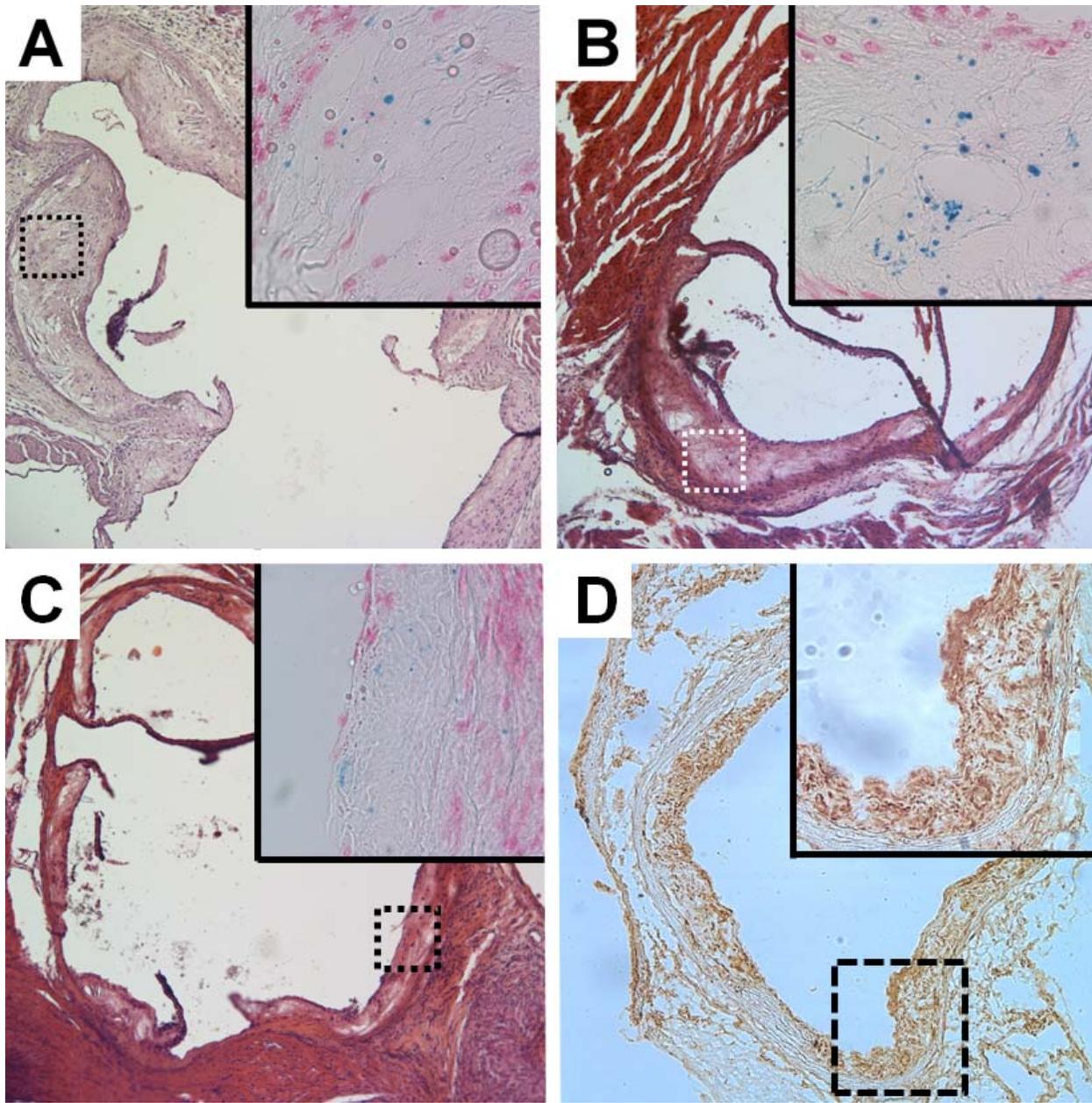
Figure 1. Histology sections. Hematoxilin-eosin staining of the aortic roots of three different mice (40x magnification) and inlays of Prussian-blue staining (high-power field: 100x,). Prussian-blue after (A) 500 µmolFe/kg and (B) 1000µmolFe/kg revealed a significant iron uptake only in mice injected a high-dose of Ferumoxtran-10. Iron uptake in the low-dose group was quantitatively slightly elevated but qualitatively more pronounced compared to NaCl injected mice (C). MAC-3 immunohistochemistry revealed numerous macrophages present in lesions of 9 months-old apoE $^{-/-}$ mice (D).

SE images. The blood–plaque contrast-to-noise ratio (CNR) was calculated a

$$CNR = \frac{\left(SI_{blood} - SI_{plaque}\right)}{SD_{noise}}$$

where SI is the signal intensity and SD the standard deviation.

2.6. Statistical analysis

Data are presented as mean ± SD. For differences between multiple groups, a one-way ANOVA test was used followed by a post-hoc Least Significance Difference test for multiple comparisons (SPSS 15.0 for windows, SPSS Inc., USA). For differences between two groups, the Student's t test was used. A value of $p < 0.05$ was considered statistically significant.
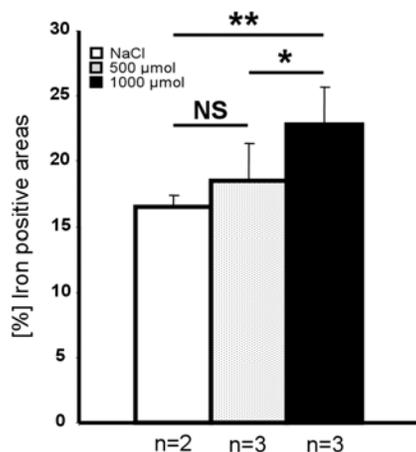
Figure 2. Histology data. Percentage of iron positive cells per high-power field >48 hours after sham-injection (white-bar), 500µmolFe/kg (grey bar) and 1000µmolFe/kg (black bar). *: p=0.099, **: p=0.045, NS: not significant..
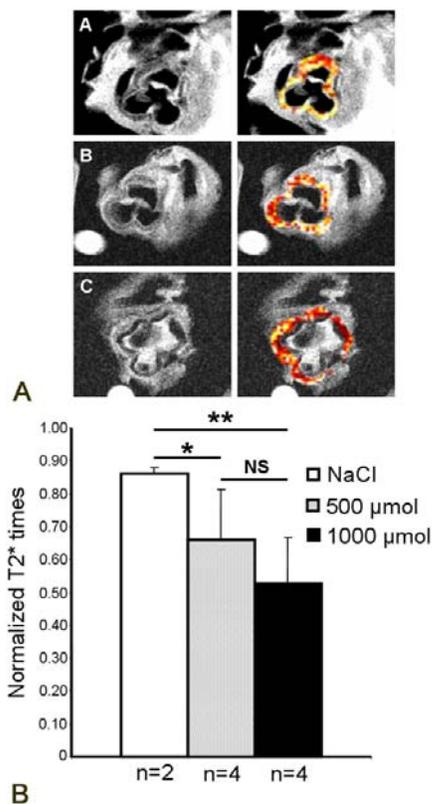

Figure 3. T2* mapping. a.) High resolution spin-echo images overlaid by T2*-maps normalized to right ventricular myocardium. Because the maximum of the overlay was set to the mean T2* of the myocardium bright spots represent normalized T2* values around 1 whereas red and black spots display regions of markedly reduced T2* values. b.) Bars showing the mean normalized T2* values in aortic roots after sham-injection (white) and the administration of 500µmolFe/kg (grey) and 1000µmolFe/kg (black) Ferumoxtran-10. *: p=0.071, **: p=0.013, NS: not significant.

3. RESULTS

3.1. Histology

Ferumoxtran-10 content in aortic roots of apoE$^{-/-}$ was not elevated after 24 hours compared to controls as measured in iron positive areas (10.85±8.62% vs. 16.48±0.85% p=NS).

Aortic roots of mice injected with Ferumoxtran-10 showed a dose dependent iron uptake after 48 hours post-contrast time as confirmed by Prussian-blue staining (Figure 1). Consequently 48 hours after 1000µmolFe/kg there was a 1.3- fold increase in iron content compared to NaCl injected mice in histology (21.4±3.8 vs. 16.5±0.9%, p=0.045). The trend toward a more pronounced iron content in the low-dose group did not reach statistically significance (p=0.099) (Figure 2) but iron staining in low-dose animals was qualitatively more pronounced than in NaCl injected mice (Figure 1).

No macrophages staining has been performed in these groups. Own data on 9 months-old apoE$^{-/-}$ mice confirmed the abundant presence of macrophages in the subintima and media with MAC-3 diaminobenzidine immunohistochemestry (Figure 1).

3.2. *ex vivo* T2* mapping

The T2* values of the myocardium did not differ significantly between the three groups (ANOVA: p=0.803). Normalized T2*-times decreased from 0.86±0.02 in controls to 0.66±0.15 after a dose of 500µmolFe/kg and 0.59±0.14 in aortic root lesions of mice injected with 1000µmolFe/Kg (p=0.038 to NaCl) (Figure 3).

3.3. *in vivo* MRI

The results obtained in *ex vivo* T2*-mapping translated into a mean of 122% increase in Plaque-to-blood CNR after the injection of 1000µmolFe/kg BW, as measured by *in vivo* MRI (Figure 4A-C). CNR on gradient echo sequences with TE=1.1[ms] increased from 6.40 to 14.23 (Figure 4D). Because of the small numbers of mice investigated we did not perform further statistical analysis.

4. DISCUSSION

This study reveals three novel findings: First we observed a dose dependent uptake of an USPIO (Ferumoxtran-10) in aortic roots of apoE$^{-/-}$ mice. Second we found that, similar to other applications, high doses of USPIOs are needed in atheroma imaging to create a significant T2* effect on *ex vivo* MR-relaxometry compared to studies in humans. Third iron-uptake shows a plateau after an incubation time ≥48 hours for at least 360 hours.

The use of untargeted iron-oxide nanoparticles in ApoE$^{-/-}$ mice has been reported in only one study so far (7). Although the elegant concept of using magneto-fluorescent nanoparticles (MFNPs) allowed the proof of iron-uptake not only by plaque macrophages but also by endothelial cells and smooth muscle cells, the used nanoparticles exhibit significant differences to clinically applicable
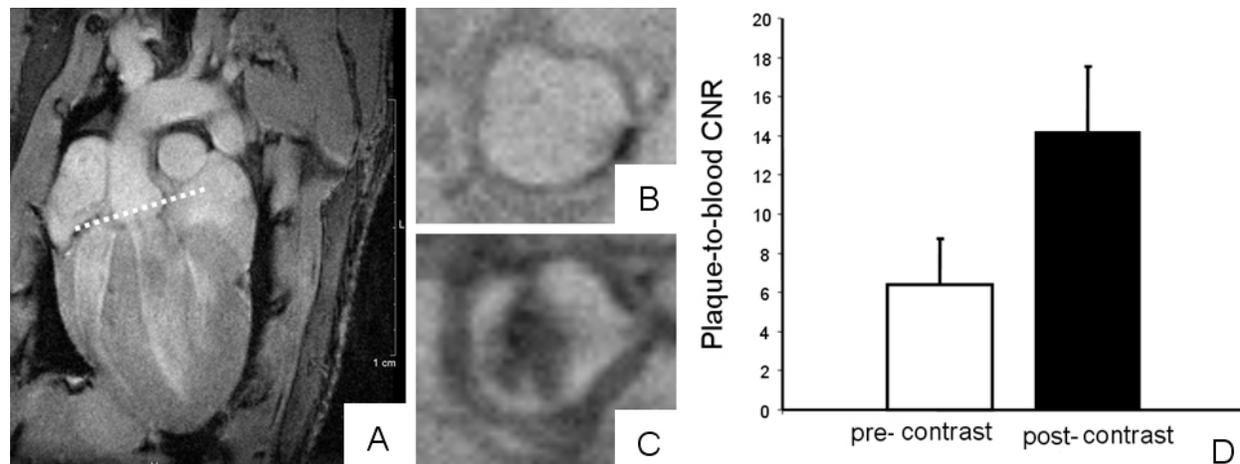
Figure 4. *In vivo* MRI. Example of *in vivo* images obtained with T2*-weighted gradient-echo sequences. The dashed line in A displays the image plane through the aortic root. Short axis slices through the aortic root pre-contrast (B) and >48 hours post-contrast (C). Plaque-to-blood CNR increases by 122% (D).

(U)SPIOs. Because of differences in size and surface properties those results may differ if USPIOs are used. These differences may explain the lower dose and incubation times used by Jaffer *et al.* compared to our study.

One report on the use of Ferumoxtran-10 in apoE$^{-/-}$ has been published currently by Joanne Morris *et al.* (11). In contrast to our study the effects of iron uptake on luminal signal loss have been observed rather the direct observations of the vessel wall. Furthermore no control group of sham-injected mice is reported and the signal loss is rather low (~0.2%). Nevertheless the doses and incubation times used in the study of Morris *et al.* are further supported by our findings.

Since human studies on atherosclerosis have utilized doses of 2.6 mgFe/kg (=46 µmolFe/kg) (12, 13) the question arises why animal studies are needed to be performed at high doses. Because of the manifold biological differences between the apoE$^{-/-}$ model of atherosclerosis and humans this issue has not been definitively answered yet but shorter half-life times in mice compared to humans have been proposed as the underlying mechanism (14). If higher-doses are applied blood monocytes are longer exposed to the contrast agent and thereby uptake should be increased as observed in *in vitro* studies (15). Since we observed a dose dependent increase in contrast, higher doses may also enhance the results in human studies (12).

Although our results are in line with prior studies on other animal models (16, 17) we are aware that the translation of our results to the clinical setting poses several problems. Nevertheless the aim of our study was to further develop the method of iron enhanced high-resolution MRI in mice because of the high diversity of possible experimental setups. So far genetical manipulation to a wider extent is only possible in mice. In contrast to other animal models of atherosclerosis no mechanical irritation of the vessel is necessary and mice are easy to keep in great numbers. Additionally iron oxide imaging might substantially improve our understanding of physiological processes and the possibilities of their pharmacological manipulation since it allows non-invasive, longitudinal studies.

In this study we observed an increase in plaque iron content in mice sacrificed 48 to 360 hours compared to aortas removed after an incubation time of 24 hours or sham-injected animals. This finding might reflect the time iron-labeled monocytes need to migrate into the atherosclerotic lesion. Studies after the injection of [^{111}In]oxine labeled monocytes yielded a half-life time of approximately 48 hours and demonstrated immigrated monocytes in atherosclerotic lesions 5 days after injection (18). In addition findings on ^{59}Fe labeled nanoparticles revealed a slow elimination and R2* values might be decreased in murine livers up to months, depending on the nanoparticles used (14, 19). Nevertheless further studies on the *in vivo* signal dynamics of iron oxides uptake in murine atherosclerosis are warranted to eventually perform longitudinal studies (20).

Some methodological issues have to be considered when interpreting our results. So far we have not investigated the effects of age and diet on the uptake of USPIOs into atherosclerotic plaques of apoE$^{-/-}$ mice. Swirski *et al.* have demonstrated an age dependent increase in monocyte infiltration into plaque macrophages until an age of 50 weeks, which matches the age of our study group. Further there was no significant effect of the diet (normal chow or high-cholesterol diet respectively) in mice aged 20 or 50 weeks (18). So it has to be hypothesized that our results may differ significantly if the experiments are performed in younger mice irrespectively of the fed diet.

The determination of T2* values is prone to external magnetic field inhomogenities und susceptibility artifacts at tissue boarders, especially at high magnetic fields. However if performed properly T2* signal decay should allow to compare USPIOs uptake irrespectively of baseline signal properties and variations in the B_1-field. The use of Fomblin to embed aortas should have minimized susceptibility differences at the vessel wall intima. To achieve comparable results the T2* times of the aortic roots were normalized to those of the right-ventricular myocardium. Unfortunately this approach inhibits quantification but corrects for differences in the external field.

The results of *in vivo* measurements are limited to pre- and post-contrast CNR comparisons rather than T2* mapping. We observed a 2.2-fold increase in blood-to-plaque CNR which was contributed by a significant increase in blood SNR in one animal. To study whether this might be due to T1 enhancing properties of a low remaining dose of Ferumoxtran-10 in the blood pool or an general increase in SNR due to variations in global measurement parameters (e.g. shim) further studies on USPIO pharmacokinetics at high injected doses are warranted.

Prussian-blue histology has been shown to lack sensitivity in regions other than spleen (21) and presumably the liver (own observations) where iron-uptake should primarily take place. Furthermore a significant amount of iron has been detected in NaCl treated animals. Possible explanations are endogeneous iron deposition (hemosiderin) (22) or sample preparation. In favor of using a contrast agent which should be clinically approved and commercially available soon we decided against the use of magneto-fluorescent nanoparticles as discussed above.

Finally no double-staining for macrophages has been performed to proof the iron deposition in plaque macrophages. Nevertheless the hypothesis of Ferumoxtran-10 uptake by macrophages has been studied numerous times (23-25).

We conclude that Ferumoxtran-10 is enriched in atherosclerotic lesions of apoE -/- mice if applied at high-doses and can be detected by *ex vivo* T2* mapping and *in vivo* gradient-echo sequences. After a time window of 48 hours plaque iron content remains unchanged for up to 2 weeks.

5. ACKNOWLEDGEMENTS

6. REFERENCES

1. Litovsky, S., M. Madjid, A. Zarrabi, S. W. Casscells, J. T. Willerson and M. Naghavi: Superparamagnetic iron oxide-based method for quantifying recruitment of monocytes to mouse atherosclerotic lesions *in vivo*: enhancement by tissue necrosis factor-alpha, interleukin-1beta, and interferon-gamma. *Circulation* 107, 1545-9(2003)

2. Simon, G. H., J. Bauer, O. Saborovski, Y. Fu, C. Corot, M. F. Wendland and H. E. Daldrup-Link: T1 and T2 relaxivity of intracellular and extracellular USPIO at 1.5T and 3T clinical MR scanning. *Eur Radiol* 16, 738-45(2006)

3. Ziener, C. H., W. R. Bauer and P. M. Jakob: Transverse relaxation of cells labeled with magnetic nanoparticles. *Magn Reson Med* 54, 702-6(2005)

4. Yablonskiy, D. A. and E. M. Haacke: Theory of NMR signal behavior in magnetically inhomogeneous tissues: the static dephasing regime. *Magn Reson Med* 32, 749-63(1994)

5. Ziener, C. H., T. Kampf, G. Melkus, P. M. Jakob and W. R. Bauer: Scaling laws for transverse relaxation times. *J Magn Reson* 184, 169-75(2007)

6. Weisskoff, R. M., C. S. Zuo, J. L. Boxerman and B. R. Rosen: Microscopic susceptibility variation and transverse relaxation: theory and experiment. *Magn Reson Med* 31, 601-10(1994)

7. Jaffer, F. A., M. Nahrendorf, D. Sosnovik, K. A. Kelly, E. Aikawa and R. Weissleder: Cellular imaging of inflammation in atherosclerosis using magnetofluorescent nanomaterials. *Mol Imaging* 5, 85-92(2006)

8. Nahrendorf, M., F. A. Jaffer, K. A. Kelly, D. E. Sosnovik, E. Aikawa, P. Libby and R. Weissleder: Noninvasive vascular cell adhesion molecule-1 imaging identifies inflammatory activation of cells in atherosclerosis. *Circulation* 114, 1504-11(2006)

9. Nakashima, Y., A. S. Plump, E. W. Raines, J. L. Breslow and R. Ross: ApoE-deficient mice develop lesions of all phases of atherosclerosis throughout the arterial tree. *Arterioscler Thromb* 14, 133-40(1994)

10. Nakashima, Y., E. W. Raines, A. S. Plump, J. L. Breslow and R. Ross: Upregulation of VCAM-1 and ICAM-1 at atherosclerosis-prone sites on the endothelium in the ApoE-deficient mouse. *Arterioscler Thromb Vasc Biol* 18, 842-51(1998)

11. Morris, J. B., A. R. Olzinski, R. E. Bernard, K. Aravindhan, R. N. Willette and B. M. Jucker: p38MAPK Inhibition Reduces Aortic Ultrasmall Superparamagnetic Iron Oxide Contrast Agent Uptake as Assessed by MRI in an Atherosclerotic Mouse Model. *Proc. Intl. Soc. Mag. Reson. Med.* 15, (2007)

12. Kooi, M. E., V. C. Cappendijk, K. B. Cleutjens, A. G. Kessels, P. J. Kitslaar, M. Borgers, P. M. Frederik, M. J. Daemen and J. M. van Engelshoven: Accumulation of ultrasmall superparamagnetic particles of iron oxide in

human atherosclerotic plaques can be detected by *in vivo* magnetic resonance imaging. *Circulation* 107, 2453-8(2003)

13. Schmitz, S. A., M. Taupitz, S. Wagner, K. J. Wolf, D. Beyersdorff and B. Hamm: Magnetic resonance imaging of atherosclerotic plaques using superparamagnetic iron oxide particles. *J Magn Reson Imaging* 14, 355-61(2001)

14. Corot, C., K. G. Petry, R. Trivedi, A. Saleh, C. Jonkmanns, J. F. Le Bas, E. Blezer, M. Rausch, B. Brochet, P. Foster-Gareau, D. Baleriaux, S. Gaillard and V. Dousset: Macrophage imaging in central nervous system and in carotid atherosclerotic plaque using ultrasmall superparamagnetic iron oxide in magnetic resonance imaging. *Invest Radiol* 39, 619-25(2004)

15. Wilhelm, C., C. Billotey, J. Roger, J. N. Pons, J. C. Bacri and F. Gazeau: Intracellular uptake of anionic superparamagnetic nanoparticles as a function of their surface coating. *Biomaterials* 24, 1001-11(2003)

16. Ruehm, S. G., C. Corot, P. Vogt, S. Kolb and J. F. Debatin: Magnetic resonance imaging of atherosclerotic plaque with ultrasmall superparamagnetic particles of iron oxide in hyperlipidemic rabbits. *Circulation* 103, 415-22(2001)

17. Yancy, A. D., A. R. Olzinski, T. C. Hu, S. C. Lenhard, K. Aravindhan, S. M. Gruver, P. M. Jacobs, R. N. Willette and B. M. Jucker: Differential uptake of ferumoxtran-10 and ferumoxytol, ultrasmall superparamagnetic iron oxide contrast agents in rabbit: critical determinants of atherosclerotic plaque labeling. *J Magn Reson Imaging* 21, 432-42(2005)

18. Swirski, F. K., M. J. Pittet, M. F. Kircher, E. Aikawa, F. A. Jaffer, P. Libby and R. Weissleder: Monocyte accumulation in mouse atherogenesis is progressive and proportional to extent of disease. *Proc Natl Acad Sci U S A* 103, 10340-5(2006)

19. Weissleder, R., G. Elizondo, J. Wittenberg, C. A. Rabito, H. H. Bengele and L. Josephson: Ultrasmall superparamagnetic iron oxide: characterization of a new class of contrast agents for MR imaging. *Radiology* 175, 489-93(1990)

20. Klug, G., E. Bauer and W. R. Bauer: Patterns of USPIO deposition in murine atherosclerosis. *Arterioscler Thromb Vasc Biol*. (in press)(2008)

21. Schroeter, M., A. Saleh, D. Wiedermann, M. Hoehn and S. Jander: Histochemical detection of ultrasmall superparamagnetic iron oxide (USPIO) contrast medium uptake in experimental brain ischemia. *Magn Reson Med* 52, 403-6(2004)

22. Bentzon, J. F., C. S. Sondergaard, M. Kassem and E. Falk: Smooth muscle cells healing atherosclerotic plaque disruptions are of local, not blood, origin in apolipoprotein E knockout mice. *Circulation* 116, 2053-61(2007)

23. von Zur Muhlen, C., D. von Elverfeldt, N. Bassler, I. Neudorfer, B. Steitz, A. Petri-Fink, H. Hofmann, C. Bode and K. Peter: Superparamagnetic iron oxide binding and uptake as imaged by magnetic resonance is mediated by the integrin receptor Mac-1 (CD11b/CD18): implications on imaging of atherosclerotic plaques. *Atherosclerosis* 193, 102-11(2007)

24. Hyafil, F., J. P. Laissy, M. Mazighi, D. Tchetche, L. Louedec, H. Adle-Biassette, S. Chillon, D. Henin, M. P. Jacob, D. Letourneur and L. J. Feldman: Ferumoxtran-10-enhanced MRI of the hypercholesterolemic rabbit aorta: relationship between signal loss and macrophage infiltration. *Arterioscler Thromb Vasc Biol* 26, 176-81(2006)

25. Raynal, I., P. Prigent, S. Peyramaure, A. Najid, C. Rebuzzi and C. Corot: Macrophage endocytosis of superparamagnetic iron oxide nanoparticles: mechanisms and comparison of ferumoxides and ferumoxtran-10. *Invest Radiol* 39, 56-63(2004)

Abbreviations: USPIO: ultrasmall superparamagnetic iron oxide, SPIO: superparamagnetic iron oxide, apoE$^{-/-}$: apolipoprotein E knock-out, NaCl: natrium chloride, TE: echo time, TR: repetition time, MRI: magnetic resonance imaging, Fe: iron, CNR: contrast to noise ratio, SNR: signal to noise ratio, r1, r2, r2*: molar T1, T2, T2* relaxivities, R2*: T2* relaxivity, PD: proton-density.

Key Words: Iron Oxides, Magnetic Resonance Imaging, Atherosclerosis, Macrophages, ApoE$^{-/-}$ mice

Send correspondence to: Wolfgang Rudolf Bauer, Josef Schneiderstrasse 2, Medizinische Klinik und Poliklinik I, Universitaetsklinik Wuerzburg, D-97080 Wurzburg, Germany, Tel: 0049-(0)931-201-0, Fax: 0049-(0)931-201-0, E-mail: Bauer_W@medizin.uni-wuerzburg.de

http://www.bioscience.org/current/vol14.htm